

# **COMBUSTION OF HYDROGEN-ENRICHED METHANE IN A LEAN PREMIXED SWIRL BURNER**

**R. W. Schefer  
Combustion Research Facility  
Sandia National Laboratories  
Livermore, CA 94551-0969**

## **Abstract**

The stability characteristics of a premixed, swirl-stabilized flame were studied to determine the effects of hydrogen addition on flame stability under fuel-lean conditions. The burner configuration consisted of a centerbody with an annular, premixed methane/air jet. Swirl was introduced to the flow using 45-degree swirl vanes. The combustion occurred within an air-cooled quartz chamber at atmospheric pressure. The results, using methane/hydrogen fuel mixtures, showed that the addition of up to 41% hydrogen significantly extended the lean burning limit. Planar Laser-Induced Fluorescence (PLIF) measurements of the OH radical were applied to study the behavior of the OH mole fraction near the lean stability limit. The results showed that as the lean stability limit was approached the overall OH mole fraction decreased, the flame width decreased and length increased, and the high OH region took on a more intermittent, shredded appearance. For operating conditions near the lean stability limit, the addition of a moderate amount of hydrogen to the methane/air mixture resulted in a significant increase in the OH concentration and a more robust appearing flame.

## Introduction

The development of advanced combustion capabilities for gaseous hydrogen and hydrogen-blended hydrocarbon fuels in gas turbine applications is an area of much current interest. Driving this interest are several current needs. One need is the cost-effective utilization of alternative fuels with a wide range of heating values. For example, low and medium heating value fuels containing hydrogen are often produced as a by-product in Coal-Gasification Combined Cycle and Fluidized Bed Combustion installations. These product gases could provide a significant source of cost-effective fuels for gas turbines. A second need is related to the recognition that ultra-lean premixed combustion is an effective approach to NO<sub>x</sub> emissions reduction from gas turbine engines. Hydrogen blended with traditional hydrocarbon fuels significantly improves flame stability during lean combustion and allows stable combustion at the low temperatures needed to minimize NO<sub>x</sub> production. A longer-term need is the desire to minimize and, eventually, eliminate UHC and CO<sub>2</sub> emissions. The use of hydrogen-blended fuels provides both a solution to the immediate need for NO<sub>x</sub> reduction, and also provides a transition strategy to a carbon-free energy system in the future.

Changes in fuel composition, particularly the addition of hydrogen to hydrocarbon fuels, affect both the chemical and physical processes occurring in flames. These changes affect flame stability, combustor acoustics, pollutant emissions, combustor efficiency and other important quantities. Few of these issues are clearly understood. A primary goal of this research is to investigate issues surrounding pure hydrogen and hydrogen-enriched hydrocarbon fuel use. Surprisingly few studies in the literature have been directed toward the effects of hydrogen addition on hydrocarbon flame chemistry and stability, and on pollutant formation under very fuel lean conditions. Relevant studies exist in the areas of spark ignition engines and gas turbine combustors. Studies in spark ignition engines clearly show the benefits of hydrogen addition. For example, Larson and Wallace (1997) showed that spark ignition engines operated on a blend of natural gas and hydrogen produced lower exhaust emissions. Meyers and Kubesh (1997) further showed that hydrogen addition to natural gas extended the lean engine operating limit.

Results in large-scale gas turbine combustors also indicate advantages to hydrogen addition. Clayton (1976) carried out an early study of the effect of hydrogen addition on aircraft gas turbines. Up to 15% hydrogen addition to JP-5 or JP-6 produced leaner blowout limits and corresponding reductions in NO<sub>x</sub> (less than 10 ppm @ 15% O<sub>2</sub>) while maintaining acceptable CO and HC emissions levels. Tests conducted in a single combustor test stand at full pressure and temperature at the GE Corporate Research and Development Center and in the field in a natural gas-fired cogeneration plant at Terneuzen, The Netherlands, demonstrated improved flame stability with hydrogen addition to natural gas fuel (Morris et al., 1998). Blends of up to 10% hydrogen by volume showed reduced CO emissions under lean conditions, and lower NO<sub>x</sub> emissions for a given CO level. The combustion of low BTU gasified fuels with up to 35% hydrogen content has also been demonstrated in an existing, low emission gas turbine with minimal modification (Ali and Parks, 1998).

## Experimental System

A schematic of the test apparatus, including the premixer and combustion chamber, is shown in Fig. 1. The inside diameter of the premixer tube is 4.1 cm and the outer diameter of the fuel

centerbody is 2.5 cm. The flame is stabilized on a centerbody with seven 45-degree swirler vanes, located at the end of the mixing chamber. The combustion chamber is a 30.5 cm long quartz tube of 8.3-cm inside diameter. Combustion air is provided by an air compressor and metered upstream of the burner using mass flow meters. The air is dried and filtered to remove particles by suitable in-line filters. The fuels, methane and hydrogen, are metered using mass flow meters. The mass flow meters are calibrated using laminar flow elements to an estimated accuracy of 2%.

A frequency-doubled, Nd:YAG-pumped dye laser provided the ultraviolet laser radiation for excitation of the OH molecule. The beam (8-ns pulse duration,  $0.3\text{-cm}^{-1}$  line width) was used to pump the Q<sub>1</sub>(8) line of the (1,0) band of the OH  $A^2\Sigma - X^2\Pi$  electronic transition at 283.556 nm. Excitation from the N''=8 level was selected to minimize the temperature sensitivity of the fractional population within the absorbing level. The laser-pumped Q<sub>1</sub>(8) line has a population fraction that varies by only 10 percent over the temperature range 1000 K to 2300 K. The collimated laser sheet for the OH fluorescence was formed by a cylindrical/spherical lens combination. The OH fluorescence signal was collected using a 105-mm focal length, f/4.5 UV Nikkor lens, passed through a colored glass filter, and focused onto an intensified CCD camera. The intensifier was gated for 400 ns, encompassing the 8-ns laser pulse, to minimize the effects of flame luminescence and background light. The camera was operated in a 512 x 512-pixel format, which provides a field-of-view of 81.9 mm x 81.9 mm with a spatial resolution of 160  $\mu\text{m}/\text{pixel}$ .

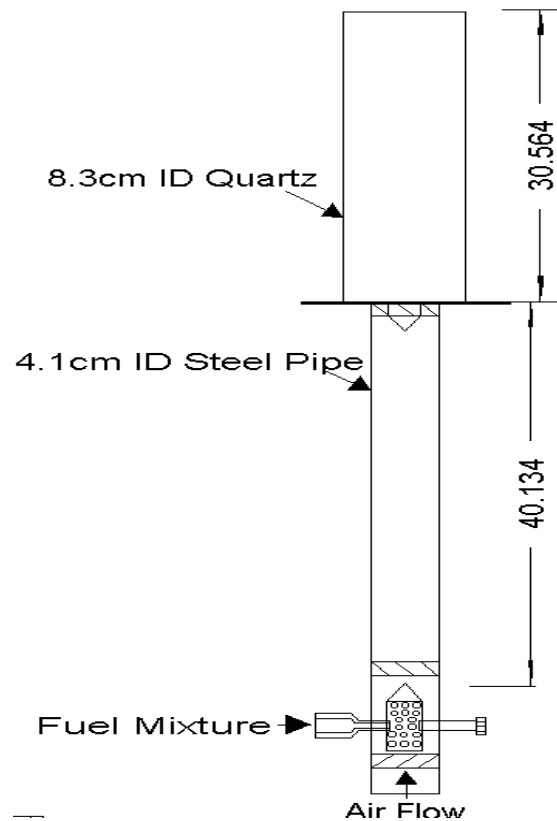
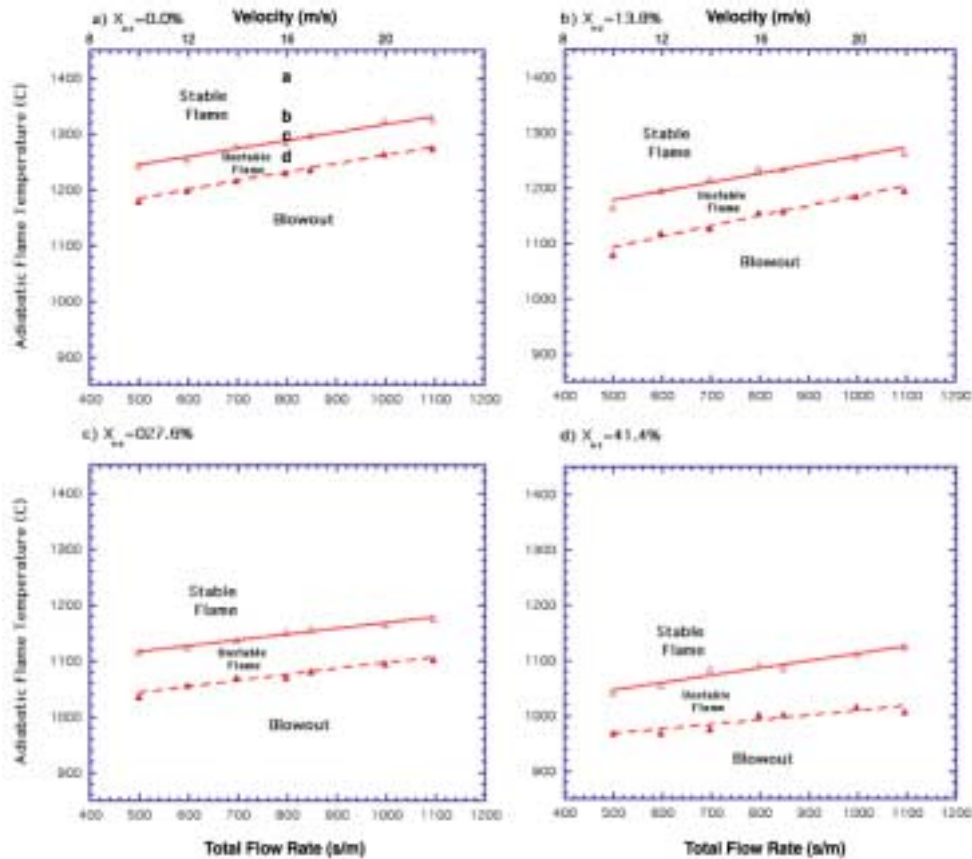


**Figure 1. Schematic of experimental swirl burner and premixer.**

## Results

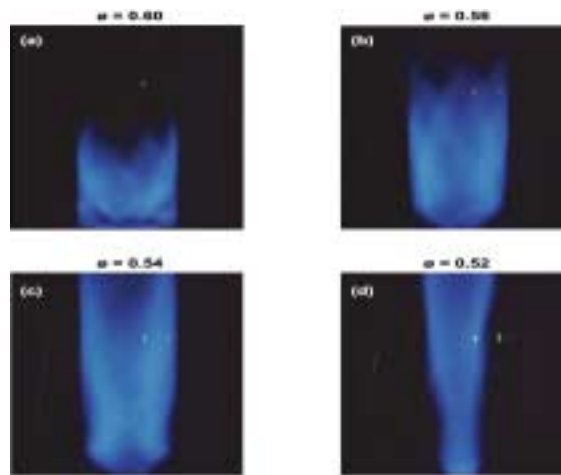
### Flame Stability

The flame stability characteristics were determined for the burner over a range of operating conditions. The resulting lean stability map is shown in Fig. 2a for methane-air flames with no hydrogen addition. The measurements in Fig. 2 were obtained by maintaining a constant total volumetric flow rate and incrementally decreasing the adiabatic flame temperature by reducing the fuel/air ratio. The adiabatic flame temperature,  $T_{ad}$ , rather than the more conventional fuel/air ratio was used as the vertical axis in Fig. 2 since burner  $\text{NO}_x$  emissions are more directly correlated with flame temperature. Note, however, that under fuel-lean conditions both  $T_{ad}$  and the fuel/air ratio increase in the same direction along the axis. Generally, the flame blew out at lower flow rates as  $T_{ad}$  was decreased, or the fuel/air ratio became leaner. The points in Fig. 2a denoted flames a through d correspond to the flame photograph sequence in Fig. 3 where the total flow rate is maintained constant while  $T_{ad}$  is decreased.



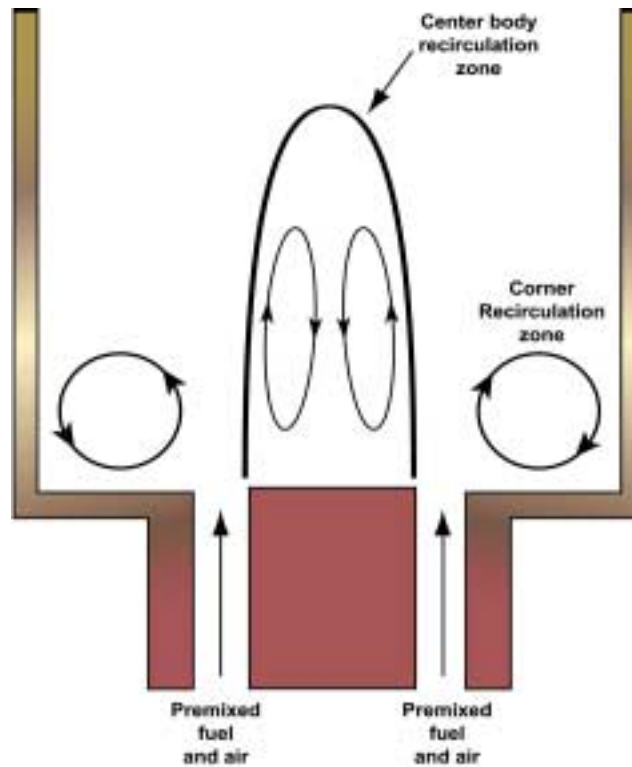
03:30:20 R8

**Figure 2. Swirl-burner flame regime and blowout map for premixed  $\text{CH}_4/\text{H}_2/\text{air}$ . a)  $X_{H_2}=0.0\%$ , b)  $X_{H_2}=13.8\%$ , c)  $X_{H_2}=27.6\%$ , d)  $X_{H_2}=41.4\%$ .**



00187-02-08

Figure 3. Direct flame luminosity photographs.  $u=14$  m/s,  $X_{O_2}=0.0$ . a)  $T_{ad} = 1385C$ ; b)  $T_{ad} = 1311C$ ; c)  $T_{ad} = 1274C$ ; d)  $T_{ad} = 1237C$



00187-02-08

Figure 4. Schematic of flow field in swirl-stabilized combustor.

A discussion of the flame behavior seen in Fig. 3 is facilitated by considering the flow field associated with this burner configuration. Figure 4 shows schematically the likely flow field based on other observations in the present flame. As shown, the flow downstream of the inlet consists of two recirculation zones. One, located downstream of the centerbody, is consistent with velocity measurements in bluff-body stabilized flows (Schefer et. al, 1987). The second is associated with the quartz confinement tube and is located in the outer corner region where the vertical confinement tube walls intersect the horizontal inlet plate. This is typically referred to as the corner recirculation zone. At the highest flame temperature of 1385C (flame a in Fig. 3a), the flame is short and blue and fills the entire quartz confinement tube in the upstream region. Note also with this flame, combustion in the corner recirculation zone is clearly indicated by the continuous flame emission originating there. Decreasing  $T_{ad}$ , visible emission from the corner zone becomes increasingly intermittent until, at  $T_{ad} = 1311C$  (flame b) there is no visible flame in the corner recirculation zone. The diameter of the flame decreases as the flame moves away from the confinement tube walls and length of the flame increases as  $T_{ad}$  is decreased until, for  $T_{ad} = 1274C$  (flame c), the flame extends past the downstream end of the quartz tube. Finally, further reductions in  $T_{ad}$  cause the flame to become unstable, oscillating between a larger-diameter flame that extends across much of the confinement tube (similar to flame c), to a much narrower flame that can best be described as a narrow cylinder extending along the center of the enclosure. Flame d at  $T_{ad} = 1237C$  is typical of this condition. The flame remains like this until, at sufficiently lean conditions, the flame becomes paler blue and eventually is extinguished. This corresponds to the flame lean blowout condition.

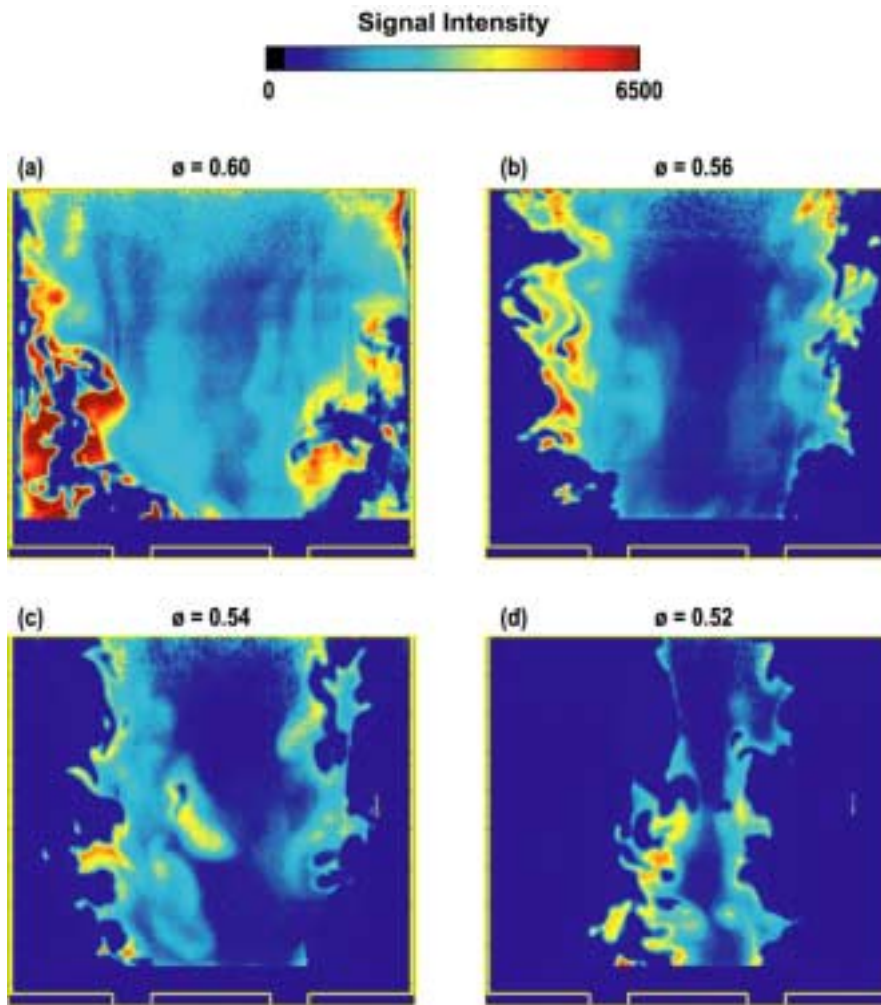
The OH PLIF images corresponding to flames a through d are shown in Fig. 5. For all equivalence ratios the outer edge of the high OH region is very irregular and probably reflects variations in the local velocity, which contort the flame surface. The OH is uniform throughout much of the flame, with locally high concentration regions forming thin filaments that typically extend along the irregular interface located between unburned reactants and combustion products.

### **Effects of Hydrogen Addition on Lean Flame Stability**

A major question in this study is the effect of hydrogen addition on flame stability under lean operating conditions. To characterize the effect of hydrogen addition on lean burner stability, various amounts of hydrogen were added to the methane/air mixture and the flame stability measurements were repeated. Also shown in Fig. 2 are the resulting lean blowout curves for 13.8%, 27.6% and 41.4% hydrogen dilution. It can be seen that hydrogen addition significantly extends the lean stability limits. For example, at a velocity of 10 m/s, the methane flame blows out at  $T_{ad} = 1170C$ . The addition of 41.4% of hydrogen extends the stable flame regime to  $T_{ad} = 1058C$ . This change represents a 10.6% reduction in  $T_{ad}$  at the lean flame stability limit.

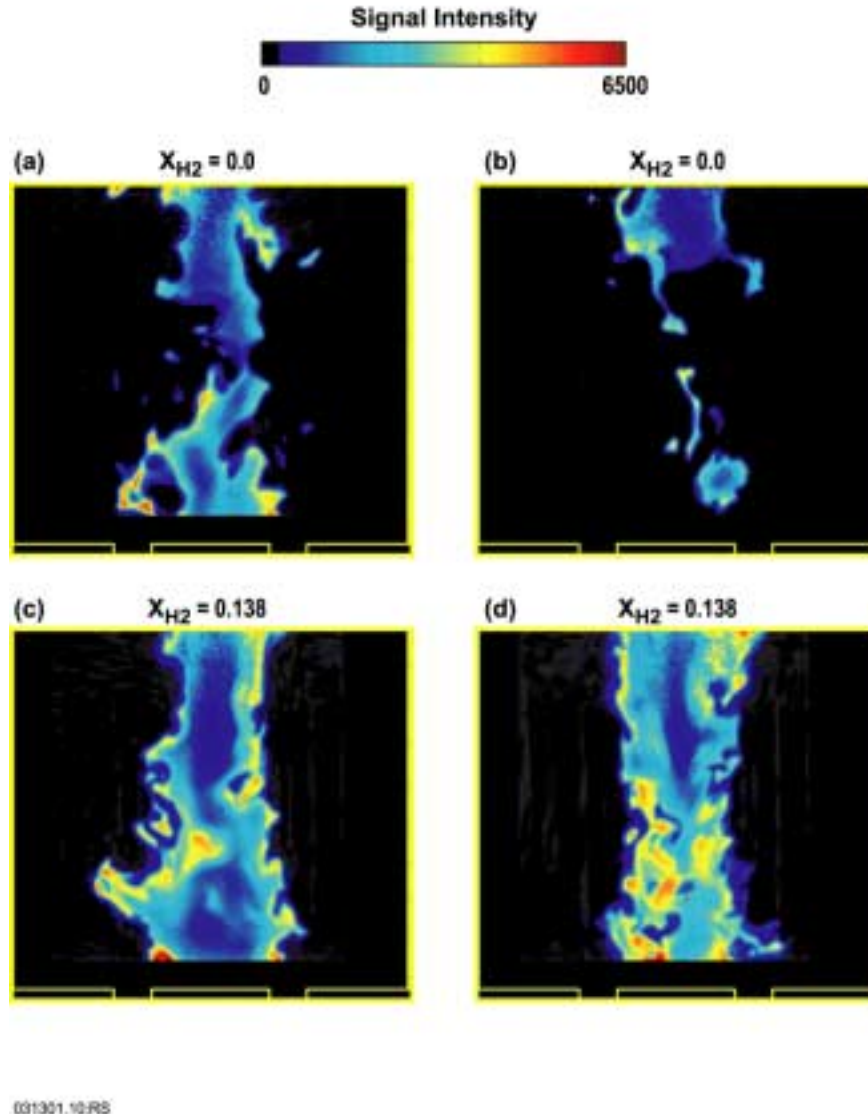
Of particular interest is the effect of hydrogen addition on the OH concentration near the lean flame stability limit. Phillips and Roby (1999) proposed that the enhanced reaction rates with hydrogen are due to an increase in the radical pool. For example, H radicals are important to flame stability because of their role in the important chain branching reaction  $H + O_2 \leftrightarrow OH + O$ . Furthermore, the reduction in CO emissions with hydrogen addition was attributed to the increased radical pool. Higher OH concentrations are likely to promote completion of CO oxidation to  $CO_2$  via the OH radical. OH PLIF images near the lean blowout limit are shown in

Fig. 6. Figures 6a and 6b show two images taken on different laser shots at  $T_{ad} = 1237\text{C}$  and an inlet velocity of 17 m/s with no hydrogen addition. This velocity is just below the blowout velocity of 18 m/s for this  $T_{ad}$ . Comparison of the two images shows the time-varying nature of the flame. Figures 6c and 6d show results for the same velocity and nearly the same  $T_{ad} = 1241\text{C}$ , but with 13.8% hydrogen addition. Comparison of these images shows that the size of the high OH region increases considerably, that the OH region is more continuous and that the peak OH levels along the outer edges of the flame are higher. Similar to the behavior with no hydrogen addition, further increases in the velocity with hydrogen added result in a narrower, elongated, and more shredded flame as blowout is approached.



031301.08 RS

Figure 5. Single-shot, OH PLIF images in swirl-stabilized flame. Same flame sequence as photographs in Fig. 4. The false color map indicates OH mole fraction. Burner inlet nozzle location is indicated at the bottom of the image.



**Figure 6. Single-shot, OH PLIF images in swirl-stabilized flame.  $u=17$  m/s. a), b)  $X_{H_2}=0.0$ ,  $T_{ad} = 1237C$ ; c), d)  $X_{H_2}=0.138$ ,  $T_{ad} = 1241C$ .**

### Time-Averaged OH Distributions

The above results emphasize the instantaneous OH distributions. Also of interest are the time-averaged OH distributions. The time-averaged OH distributions for  $X_{H_2}=0.0$ , 0.138 and 0.414 are shown in Fig. 7. At these flow conditions, for no hydrogen addition there is no flame in the corner recirculation zone. With the addition of hydrogen the OH extends upstream into the corner recirculation zone along a layer adjacent to the inner wall of the quartz tube. Increasing the hydrogen addition from 0.138 to 0.414 results in the OH concentration extending across a slightly wider fraction of the corner recirculation zone.



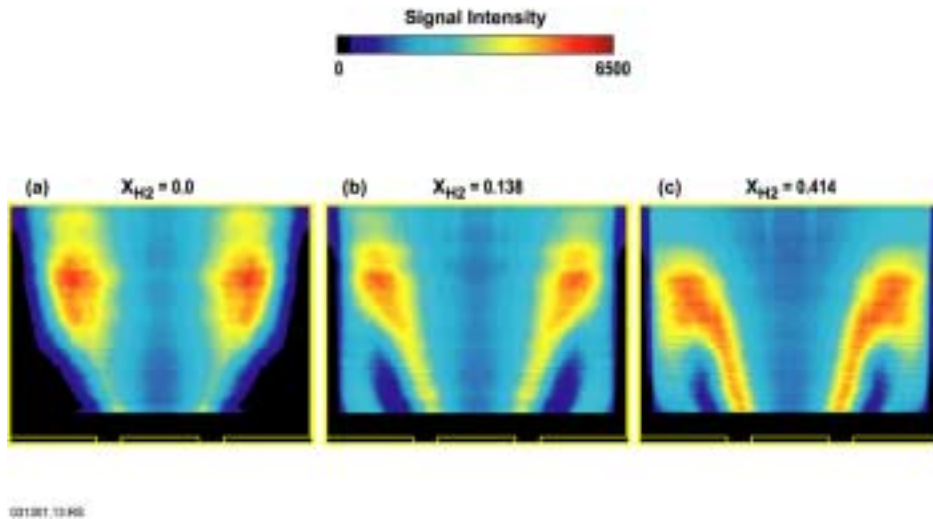


**Fig. 7. Time-averaged OH PLIF images in swirl-stabilized flame.  $u=14$  m/s.**  
 a)  $X_{H_2}=0.0$ ,  $T_{ad} = 1274C$ ; b)  $X_{H_2}=0.138$ ,  $T_{ad} = 1280C$ ; c)  $X_{H_2}=0.414$ ,  $T_{ad} = 1303C$ .

As with the three flames shown in Fig. 7, the effect of hydrogen addition considerably alters the global flame characteristics and makes direct comparisons of the OH levels difficult. To minimize this problem, flow conditions were determined where the hydrogen addition could be varied while maintaining the same global flame characteristics. It was found that for  $u=14$  m/s and  $T_{ad} \approx 1250C$ , hydrogen addition could be increased from 0% to 13.8% while maintaining a flame similar to that shown in Fig. 7 a). That is, no flame in the corner recirculation zone and a flame that has moved away from the quartz walls. Time-averaged radial profiles corresponding to these conditions are presented in Fig. 8. They show that an increase in the hydrogen from 0% to 13.8% causes nearly a 44% increase in the maximum OH. Other data shows that a subsequent increase from 13.8% to 41.4% hydrogen results in a much smaller 4% increase in the maximum OH.

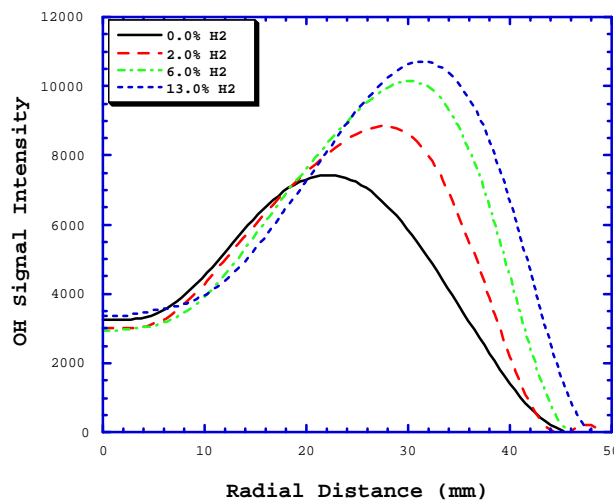


**Figure 8. Radial profiles of OH intensity for different hydrogen addition at  $y=40$  mm.  $u=14$  m/s,  $T_{ad} = 1250C$ .**

## Conclusions

PLIF measurements of the OH radical were made to understand the effects of hydrogen enrichment on methane flames near lean blow out. Both instantaneous and time-averaged data were measured. The lean stability limit was lowered by the addition of hydrogen to the fuel, as expected. This improved stability with hydrogen enrichment is postulated to be a direct result of increasing the H, O, OH radical concentrations, which increases several key reaction rates. Results showed that moderate amounts of hydrogen enrichment led to significant increases in the OH radical concentrations. Specifically, the addition of up to 13.8% hydrogen causes a 44% increase in the maximum OH concentration, while further increases result in only marginally higher radical concentrations for the conditions tested.

## Acknowledgments

This research was supported by the U. S. Department of Energy Hydrogen Program.

## References

- Ali, S. A. and Parks, W. P. 1998. "Renewable Fuels Turbine Project." ASME Paper 98-GT-295.
- Clayton, R. M. 1976. "Reduction of Gaseous Pollutant Emissions from Gas Turbine Combustors using Hydrogen-Enriched Jet Fuel—A Progress Report." NASA TM 33-790.
- Larsen, J. F. and Wallace, J. S. 1997. *J. Engineering for Gas Turbines and Power*, 119: 218-226.
- Meyers, D. P. and Kubesh, J. T. 1997. *J. Engineering for Gas Turbines and Power*, 119: 243-249.
- Morris, J. D., Symonds, R. A., Ballard, F. L. and Banti, A. 1998. "Combustion Aspects of Application of Hydrogen and Natural Gas Fuel Mixtures to MS9001E DLN-1 Gas Turbines at Elsta Plant, Terneuzen, The Netherlands." ASME Paper 98-GT-359.
- Phillips, J. N. and Roby, R. J. 1999. "Enhanced Gas Turbine Combustor Performance Using H<sub>2</sub>-Enriched Natural Gas." ASME Paper 99-GT-115.
- Schefer, R. W., Namazian, M. and Kelly, J. 1987. "Velocity Measurements in a turbulent Nonpremixed Bluff-Body Stabilized Flame." *Combust. Sci. Technol.*, 56: 101-138.